



Extinction of non-equidiffusive premixed flames with oscillating strain rates



Aditya Potnis^a, Vishnu R. Unni^a, Hong G. Im^b, Abhishek Saha^{a,*}

^a Department of Mechanical and Aerospace Engineering, University of California San Diego, La Jolla, CA 92093, United States

^b Clean Combustion Research Center, King Abdullah University of Science and Technology, Thuwal, Saudi Arabia

ARTICLE INFO

Article history:

Received 21 February 2021

Revised 16 July 2021

Accepted 19 July 2021

Available online 19 August 2021

Keywords:

Extinction

Differential diffusion

Unsteady strain rate

ABSTRACT

Extinction of premixed flames under non-uniform, unsteady strain is a phenomenon commonly observed in turbulent combustors. To assess the role of inequity in thermal and mass diffusion, represented by a global Lewis number (Le) - defined as the ratio of the mixture's thermal diffusivity to the mass diffusivity of the deficient species, on such extinctions, we present a study of counterflow twin-flames with various Le under oscillating strain rates. Experimental results confirm that for low mean strain rates, the amplitude of strain rate oscillation required for extinction is so large that the flow temporarily alters its direction, leading to distortion of the counterflow flow-field, destabilization, and eventual extinction of the flame irrespective of Lewis number. However, for relatively large mean strain rates, extinction results from flame-response to the peak instantaneous strain rate. For $Le > 1$ mixtures, the maximum strain rate that the flames can sustain is greater than the steady state extinction values, while $Le \leq 1$ flames extinguish at a maximum strain rate, approximately equal to the steady state strain condition. This distinctively disparate behaviors of extinctions depending on the Lewis number are analyzed and delineated using numerical simulations of unsteady flames.

© 2021 The Author(s). Published by Elsevier Inc. on behalf of The Combustion Institute. This is an open access article under the CC BY license (<http://creativecommons.org/licenses/by/4.0/>)

1. Introduction

The role of flow non-uniformity in the dynamics of laminar flames is a topic of great interest owing to its fundamental as well as practical relevance to a variety of combustion phenomena including the modeling of turbulent combustion. The propagation of premixed turbulent flames, which are often represented as a collection of elemental laminar flames, known as flamelets, is controlled by the collective behavior of these flamelets [1–3]. Turbulence is realized as local flow non-uniformities or disturbances, hence understanding the influence of these disturbances on the behavior of laminar flamelets is critical in the development of robust turbulent combustion models.

The flow non-uniformities present upstream of the propagating flames are often quantified by strain rates (K), and are known to have a strong influence on flames, particularly for mixtures with differential diffusion, a phenomenon quantified by non-unity Lewis number, Le . Lewis number is defined as the ratio of thermal diffusivity of the mixture to the mass diffusivity of the deficient species. Experiments and complementing theoretical analyses

on the response of a laminar flame to changes in strain rate confirmed that flames are strengthened with increasing positive strain rates if $Le < 1$, and weakened if $Le > 1$ [3–11]. This discovery subsequently led to a series of studies in which the propagation speed, flammability limit and extinction conditions for non-equidiffusive mixtures were quantitatively studied [9,12]. In particular, the role of (positive) strain on flame extinction received extensive attention due to its significance in determining reliable operating conditions and safety limits of practical devices. A series of experimental, numerical and theoretical studies using a canonical stagnation flow, and counterflow burners, have shown that for $Le > 1$ mixtures, a progressive quasi-steady increase in strain rate K reduces the heat release rate. This in turn decreases the flame temperature due to modification in reaction rate, leading to a progressively weaker flame, and as such the flame extinguishes at a critical strain rate known as extinction strain rate, K_e . For $Le < 1$ mixtures, the flame temperature and heat release rate increase with strain rate and as a result, the flame becomes stronger at higher strain rates, until the flame movement is arrested as it reaches the stagnation surface [13,14]. Subsequently, with increase in strain rate, the residence time for the flow across the flame is reduced, leading to incomplete reaction, reactant leakage and reduction in the flame temperature. Hence, the flame extinguishes beyond a critical strain

* Corresponding author.

E-mail address: asaha@eng.ucsd.edu (A. Saha).

rate K_e . It is to be noted that, although the $Le \approx 1$ flames are insensitive to increase in K , the extinction of these flames also occurs close to stagnation plane due to lack in residence time [15]. Such dichotomy of flame extinction behavior for $Le > 1$, and ≤ 1 mixtures is often presented in form of the well-known S-curve where the flame response is plotted as function of the Damköhler number, defined as the ratio of flow timescale vs. reaction timescale [15].

While the research mentioned above is concerned with quasi-steady strain rates, flows in practical systems are often inherently unsteady and possibly turbulent. Several studies with unsteady strain rates showed that the response of a flame in an oscillating flow field depends on the frequency and amplitude of the oscillation as well as the mean strain rate [16–19]. In particular, for low frequency oscillations, the flame is quasi-steady and readily responds to the imposed perturbations. On the other hand, for sufficiently high frequencies the flame fails to respond in adequate time to the rapid fluctuations in the incoming flow and hence, the response is attenuated. For very high frequencies, the flame is invariant to oscillations. This behavior of flame response has been described by using the Strouhal number, and Stokes parameter, as measures of flow time scale versus perturbation timescale [17,18,20–27]. Furthermore, it was also shown that the response in heat release rate, in general, has a phase lag with the oscillation in strain rate. Owing to the facilitating and inhibiting effects of strain rates, the lag in heat release rate response is close to 0 and π for $Le < 1$ and > 1 mixtures, respectively [28]. It is also noted that some numerical studies demonstrated that the flame responds to unfavorable conditions and extinguishes only if they persist for a minimum amount of time [29,30]. Subsequently, studies [31,32] assessed the number of cycles of oscillations in strain rate required before flame extinction can be achieved and reported that this number depends on the oscillation amplitude, and frequency.

While previous literature has delved into characterizing the effect of oscillating strain rate on flame extinction in general, a detailed study into the determination of extinction strain rate limits for unsteady $Le > 1$ and ≤ 1 flames has not been conducted. It is critical to characterize the effect of differential diffusion on the range of strain rate oscillations which flames can withstand and hence, shed light on possible extension of the flammability limits. Such studies will, subsequently, be able to provide insights in constructing flamelet directories used in modeling turbulent flames, which are traditionally derived based on flames under steady strain rates [33]. Recognizing its importance and criticality, we, herein, present a systematic experimental determination of the extinction conditions for counterflow twin flames with non-unity Le subjected to oscillating (positive) strain rates. Additionally, by using numerical simulation we elucidate the unsteady behaviour of these flames at selected conditions. In particular, we demonstrate how differential diffusion or Le limits the maximum strain rate a flame can be subjected to for a range of mean strain rates. We shall now present the details of the experiments, which will be followed by sections detailing the key finding from the experiments, numerical simulations and discussions, and finally a concise summary.

2. Methods and procedures

2.1. Experimental methodology

A counterflow burner with two identical 15 mm diameter nozzles with a separation distance (L) of 20 mm was operated in the twin flame configuration (Fig. 1a). Premixed gas at equal flow rates was supplied to both nozzles; the ensuing two flames stabilized symmetrically on each side of the stagnation plane. Gaseous fuels were used along with oxidizer (O_2) and inert nitrogen (N_2). Three

programmable mass flow controllers were used to modulate the individual flow rates of fuel, O_2 and N_2 to achieve the total flow rate with desired mixture ratios required for non-unity Le flames. A separate N_2 co-flow was used to envelope the premixed gas and flame from the ambient and hence, alleviate any possible influence of surrounding air on flame dynamics. The co-flow was critical to achieve repeatable and reliable measurement of extinction conditions, which can easily be affected by ambient air entrainment causing alteration in the mixture composition. A schematic of the various components of the burner along with a typical flow field are shown in Fig. 1a.

To produce an oscillating strain rate, two speakers (acoustic drivers) were mounted at the end of plenum chambers on each side of the counterflow setup (Fig. 1a). The speakers were driven by a sinusoidal voltage signal, generated using a function generator (direct digital synthesis, DDS, signal generator from Koolertron) along with an amplifier. Using Fast Fourier Transform (FFT) of the time dependent oscillating flow velocity at the nozzle exit, the mean, amplitude, and frequency of the flow velocity and resulting strain rate were measured. The global strain rate of a symmetric twin-flame configuration, is defined as, $K = 4V/L$, where V is the mean flow velocity from each nozzle at the central axis, and L is the separation distance between the nozzles [34,35]. The sinusoidal oscillations of the strain rate can be expressed as, $K(t) = \bar{K} + K_0 \sin(2\pi ft)$ where \bar{K} , K_0 and f are the mean, amplitude, and frequency of the strain rate oscillations. Here, we note the counterflow setup is designed to study flames under positive strain rate, thus in our study $K > 0$.

The flow field was visualized and characterized using Particle Image Velocimetry (PIV) on the cold flow without the presence of flame. A dual pulsed Nd:YLF laser (wavelength 527 nm) coupled with a set of sheet-making optics was used to create a 1 mm thick vertical laser sheet, which was so positioned that it passed vertically through the center of the burner. The flows exiting both nozzles were seeded with D.E.H.S. (di-ethyl hexyl sebacate) droplets with a mean size of 1–2 μm . A high speed (Phantom V710) camera connected to combination of a 27 mm extension tube, Nikon Teleconverter (2x magnification) and a AF-S Nikkor 28–70 mm lens was placed orthogonal to the laser plane to capture Mie scattering images, which were subsequently processed using LaVision's Davis 10 software to obtain the velocity field. Furthermore, the flame dynamics and flame extinction were identified through direct imaging (sample images shown in Fig. 2 using the same camera setup, for identification of flame location for both steady, and oscillating strain rates. For PIV, the images were recorded at a rate of 10,000 frames per second using $1200 \times 800 \text{ px}^2$ window, at a spatial resolution of $\approx 0.038 \text{ mm/px}$. The conditions (flow rates, amplitude and frequency of speakers) required for extinction of flame were recorded through repeated experiments with reacting flow. Subsequently, PIV was performed at the same condition of flow in the absence of flame, to determine the velocities at the nozzle exit and furthermore, the corresponding strain rates. A typical steady state center-line axial velocity for non-reacting flow is shown in Fig. 1b.

To demonstrate that the observed flame dynamics are independent of fuel, two different gaseous fuels, methane (CH_4), and propane (C_3H_8), were used in the experiments. For each of the fuels, CH_4 , and C_3H_8 , two mixtures with different Le were used. The flame nomenclature and corresponding mixture conditions are tabulated in Table 1. The table also states the calculated effective Lewis number for methane and propane flames as reviewed by Matalon [36]. To assess the true values of Le , a qualitative yet direct assessment can be performed of the change in flame speed (S_u) or burning rate ($\rho_u S_u$) with strain rate. As shown in Fig. 3, the normalized burning rate, $\rho_u S_u / \rho_0 S_L$ (where $S_u = u|_{\max(q)}$, i.e. the flow velocity at the location of maximum heat release rate as referenced by Egolfopoulos et al. [37] for the rich methane flame (Flame 1)

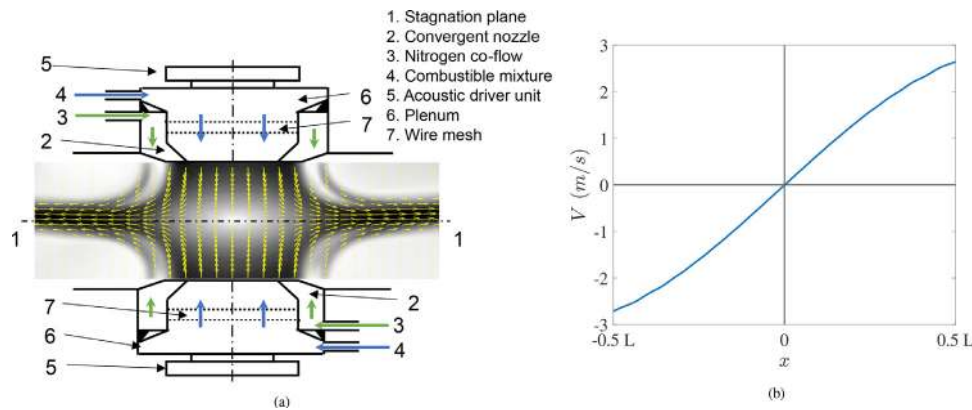


Fig. 1. a) Schematic of experimental setup showing velocity vectors for steady state operation. b) Centre-line axial velocity (V) profile as a function of distance from stagnation plane (x) for non-reacting flow at 525 s^{-1} .

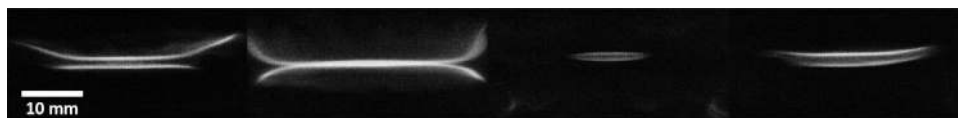


Fig. 2. Snapshots of chemiluminescence from experiments for $Le > 1$ and Flame 3 (C_3H_8) with 50 Hz forcing for normalized maximum strain rate, $K_m/K_e = 1.31$, and normalized mean strain rate, $\bar{K}/K_e = 0.98$ acquired at 700 frames per second.

Table 1

Mixture composition of flames and Recorded strain rate for steady state extinction from experiments and numerical simulation; where, Φ is equivalence ratio, $\text{O}_2\%$ is oxygen percentage molar concentration in oxidizer, T_b is adiabatic temperature of unstretched laminar flame, S_L is flame speed of unstretched laminar flame, δ_F is flame thickness of unstretched laminar flame, t_F is flame timescale of unstretched laminar flame (δ_F/S_L), K_e is experimentally obtained steady state extinction stretch rate. The uncertainty in measurement of K_e is about $\pm 10 \text{ s}^{-1}$. Ka_e is extinction Karlovitz number, defined as the ratio of flame time scale, t_F and flow time scale, $1/K_e$. Le_{eff} is effective Lewis number based on definition by Matalon [36]. Unstretched laminar flame properties were evaluated using Chemkin's PREMIXED package. *: For Hydrogen flames K_e (and thus Ka_e) was obtained only through simulations.

Name	Le	Fuel	Φ	$\frac{\text{O}_2}{(\text{O}_2+\text{N}_2)}\%$	T_b (K)	t_F (ms)	K_e (1/s)	Ka_e	Le_{eff}
Flame 1	1.11	CH_4	1.2	18	1953	4.25	304	0.775	1.07
Flame 2	0.97	CH_4	0.7	18	1670	10.38	382	0.251	0.99
Flame 3	1.88	C_3H_8	0.675	21	1843	2.11	395	1.149	1.75
Flame 4	1.05	C_3H_8	1.2	15.5	1830	2.87	567	0.613	1.24
Flame 5	1.98	H_2	4.0	12	1295	1.72	402*	1.449*	1.98
Flame 6	0.33	H_2	0.45	12	1074	28.2	518*	0.068*	0.33

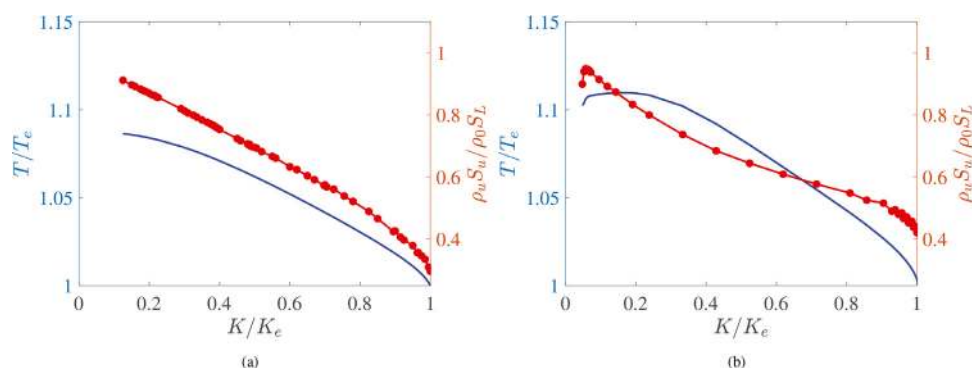


Fig. 3. Steady state flame characteristics of (a) Flame 1 and (b) Flame 2 simulated by OPUS; Normalized flame temperature T/T_e ; normalized with steady state extinction temperature (T_e), and normalized burning rate ($\rho_u S_u / \rho_0 S_L$) as functions of normalized strain rate K/K_e , normalized with steady state extinction strain rate (K_e).

decreases with increase in positive strain rate, which is hallmark of $Le > 1$ flames. On the other hand, $Le < 1$ flames show opposite behaviour as seen with the increase in burning rate for low strain rates for the lean CH_4 flame (Flame 2). Note that, the weakening of Flame 2 starts even at low strain rate and as such both burning flux and flame temperature start decreasing. Similar simulations with propane flames show that Flame 3 and Flame 4 show $Le >$ and ≤ 1 behaviors, respectively.

2.2. Details of numerical simulations

In this study, we used one-dimensional numerical simulations to assess critical flame behavior in both steady and unsteady conditions. The *Opposed-Flow Unsteady Flames* (OPUS) code developed by Im et al. [38] was used to simulate the unsteady flame response. The OPUS package is an unsteady extension of the Chemkin's OP-PDIF module [39] by incorporating DASPK [40] to solve the stiff

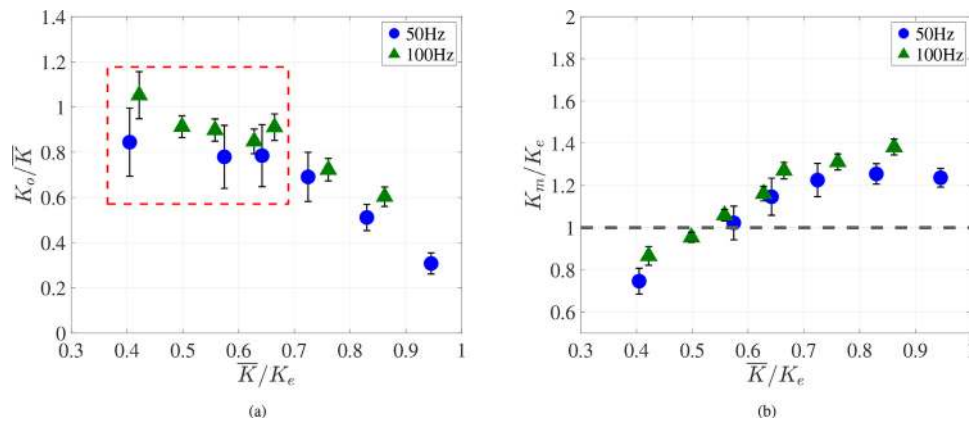


Fig. 4. Rich CH₄ (Flame 1) with $Le > 1$: (a) Normalized oscillating strain rate, K_o/K_e as a function of normalized mean strain rate \bar{K}/K_e , – denotes data points corresponding to flow reversal. (b) Normalized maximum strain rate, K_m/K_e as a function of normalized mean strain rate \bar{K}/K_e , – – denotes steady state extinction strain rate normalized by itself. Here the error bars represent the extent of standard deviation about the mean value.

system of differential-algebraic equations (DAE) using an adaptive time stepping based on the backward differentiation formula (BDF) [41]. The code employs the evaluations of detailed chemical kinetic mechanism [42] and transport properties [43]. A mixture-averaged diffusivity model was employed, and secondary effects (Soret and Dufort effects) as well as the thermal radiation effects were neglected. GRI-Mech 3.0 [44] reaction mechanism and the associated transport and thermodynamic libraries were used for all flame conditions. Additional details about the OPUS package and studies of its validation can be found in previous works [19,38,45–51] as cited here.

The spatially symmetric configuration (equivalent of twin flame configuration) with domain size of 1 cm (half of separation distance between nozzles) discretized with a fixed uniform grid of 501 points was used for the counter flow simulations in OPUS. For the unsteady simulations, a sinusoidal velocity inlet condition was imposed at the nozzle, and the frequency (f), amplitude (K_o) and mean (\bar{K}) strain rate of the ensuing condition were modulated. Each condition was simulated for a long duration to ensure that the flame settled into a stable limit cycle without exhibiting extinction. This duration was chosen as $> 10/f$, which is more than 10 times of flow-through and flame timescales. As in the experimental conditions, the simulations were conducted with a system pressure and inlet temperature of 1 atm and 300 K, respectively.

3. Experimental results

3.1. Steady state extinction

To record the steady state extinction strain rate, K_e , first, a stable twin-flame was established at a low strain rate ($\approx 209 \text{ s}^{-1}$) with the aid of an igniter. After ignition, the initial separation between the twin-flames was $\approx 5 - 7 \text{ mm}$. Once the twin-flame stabilized in the presence of co-flow, the flow rate for the main nozzles was increased in steps of approximately 1 SLPM per 2 seconds such that the flame had sufficient time to stabilize after each increment, simulating a quasi-steady process. The location of the two flames is controlled by the kinematic balance between the flow velocity, and the local flame speed, and with increase in strain rate (or flow rate) the flames migrate towards the stagnation plane [15]. As inferred from the standard S-curve for the $Le > 1$ flames, as the strain rate approaches extinction strain rate [13,14], the flame becomes weaker with progressively lower flame temperature, thus relocates closer to the stagnation plane and eventually extinguishes some distance from it. Here, the steady state extinc-

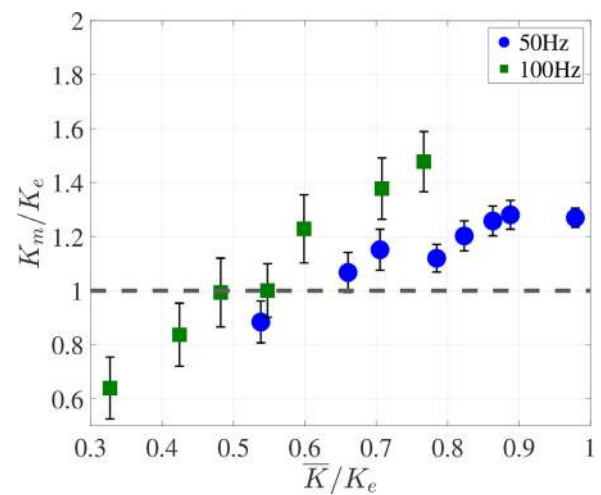


Fig. 5. $Le > 1$ and Flame 3 (C₃H₈): Normalized maximum strain rate, K_m/K_e as a function of normalized mean strain rate \bar{K}/K_e , – – denotes steady state extinction strain rate normalized by itself. Here the error bars represent the extent of standard deviation about the mean value.

tion strain rate, K_e , was defined as the maximum strain rate for which a stable flame was observed. An observation from experiments, showed that at strain rates slightly below K_e , the outer edge of the flame exhibited periodic local extinction and re-ignition, and a further small increase in strain rate led to global extinction.

The $Le < 1$ flame, on the other hand, becomes stronger as the strain rate is increased. The continuous increase in strain rate, pushes the flame to the stagnation surface and as such immobilizes it. Indeed, at high strain rate the twin flames were seen to merge at the stagnation plane and become visually indistinguishable from each other. Further increase in the strain rate was promptly followed by extinction. For all $Le \leq 1$ flames, the recorded extinction strain rate was higher than their $Le > 1$ counter-parts. Note that the Le of Flame 2 and Flame 4 is close to unity. But as stated before, the mechanism for extinction of these flames is similar to $Le < 1$. The values for K_e for the flames investigated are tabulated in Table 1.

3.2. Extinction with oscillations

The following procedure was followed to investigate the effect of oscillating strain rate on the extinction of non-equidiffusive flames. First, a twin-flame was established as described in

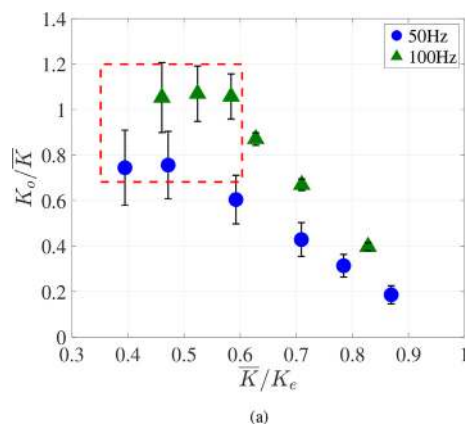
Section 2.1, subsequently the flow was adjusted to a fixed mean strain rate \bar{K} . Thereafter, using the speakers a sinusoidal perturbation of the flow was generated and modulated with the aide of the signal generator. At a fixed frequency (f), the amplitude of the signal, and hence of the strain rate oscillation, was increased in a quasi-steady process (in steps of $\approx 10 \text{ s}^{-1}$) until extinction was achieved. The amplitude of the strain rate perturbation (K_o) at the state of extinction, and the maximum instantaneous strain rate, $K_m = \bar{K} + K_o$, were recorded for a fixed f and \bar{K} . This process was repeated for a range of mean strain rate, $0.3K_e < \bar{K} < K_e$ and for multiple frequencies. Since the acoustic driver unit cannot produce a perturbation of sufficient magnitude to cause a significant oscillation in the flow at low frequencies (approximately $f < 20 \text{ Hz}$), we used $f \geq 50 \text{ Hz}$ to avoid any uncertainties. For $f > 150 \text{ Hz}$ it was observed that the flames responded to imposed oscillations but due to the limitation in acoustic driver, a large enough oscillation could not be generated to extinguish the flame. Since we are interested mostly in extinction conditions, we limit our study to lower frequencies. We will illustrate later, the trends seen in $Le \leq 1$ and > 1 flames are consistent across multiple lower frequencies and mixture conditions. For $f > 500 \text{ Hz}$, the perturbation time scale becomes comparable to that of the characteristic time scale of the flame, defined as the ratio of laminar planar flame thickness and the laminar planar flame speed, and hence flame response progressively becomes weaker for the flow oscillations at higher frequencies [16,31,52–54].

In the following subsections, we report the extinction strains rates under oscillating flow for two different Le mixtures. Next, we discuss the observed extinction behavior for $Le >$ and ≤ 1 flames under periodic oscillation of strain rates at various \bar{K} and f .

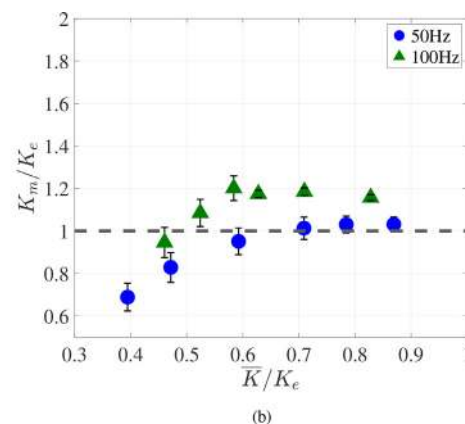
3.2.1. $Le > 1$ flames

The amplitude of the strain rate oscillation required for extinction, K_o , (normalized by the mean strain rate \bar{K}) for Flame 1, (rich methane flame with $Le > 1$), is plotted as a function of the mean strain rate, \bar{K} , normalized by the steady state extinction strain rate K_e , in Fig. 4a. We observe that, for all frequencies and at mean strain rate in the lower range of ($\bar{K}/K_e < 0.7$), the normalized amplitude of strain rate needed for extinction (K_o/\bar{K}) is almost constant, and close to unity. At larger mean strain rates ($\bar{K}/K_e > 0.7$), however, K_o/\bar{K} decreases monotonically.

Such dichotomy in the behavior of K_o/\bar{K} can be explained by assessing the uniformity in flow directions emanating from the nozzles. In particular we note that, for $K_o/\bar{K} \approx 1$, the amplitude of the velocity oscillation at the nozzle exit approaches the mean flow velocity and as such the minimum velocity during the cycle ap-



(a)



(b)

Fig. 6. $Le \leq 1$ and Flame 2 (CH_4): (a) Normalized oscillating strain rate, K_o/K_e as a function of normalized mean strain rate \bar{K}/K_e , — denotes data points corresponding to flow reversal. (b) Normalized maximum strain rate, K_m/K_e as a function of normalized mean strain rate \bar{K}/K_e — — denotes steady state extinction strain rate. Here the error bars represent the extent of standard deviation about the mean value.

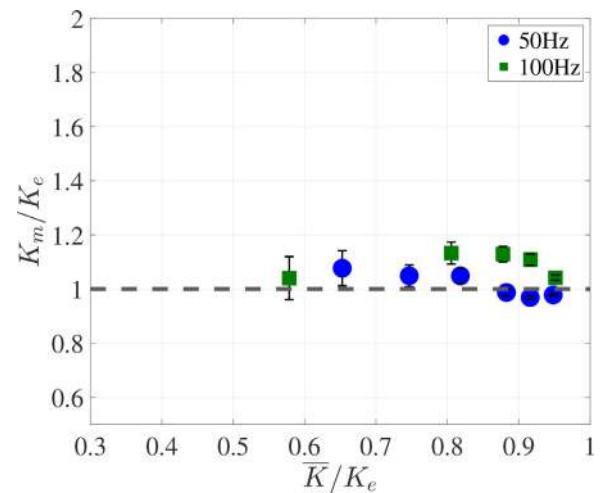


Fig. 7. $Le \leq 1$ and Flame 4 (C_3H_8). Normalized maximum strain rate, K_m/K_e as a function of normalized mean strain rate \bar{K}/K_e , — — denotes steady state extinction strain rate normalized by itself. Here the error bars represent the extent of standard deviation about the mean value.

proaches zero. Furthermore, cycle to cycle variations (shown as the error bar in Fig. 4a) may cause the amplitude of velocity oscillation to temporarily exceed unity, causing the flow direction to reverse for a short duration of the sinusoidal cycle, a phenomenon often referred to as *flow reversal* [19,29]. When *flow reversal* occurs, the canonical configuration of the counterflow flame is destroyed, and the kinematic balance between the flow velocity of the fresh mixture and flame propagation speed is disturbed, which induces a rapid and significant distortion of the flame shape and structure subsequently leading to a loss in stability, and extinction. Such extinction due to loss of stability, hereafter referred to as *extinction due to flow reversal*, is observed at low mean strain rates $\bar{K}/K_e < 0.7$ for all frequencies of oscillation studied for Flame 1 as identified in Fig. 4a. We note that, the *extinction due to flow reversal* is not a result of peak strain rate, and as such is a limitation commonly observed in counterflow setups with high amplitudes of oscillations of flow velocities. We will also show that such extinction at low mean strain rate occurs irrespective of Le and fuel. As shown in Fig. 4a, for larger mean strain rate, the normalized amplitude at extinction, K_o/\bar{K} , decreases as the \bar{K}/K_e increases. For these flow conditions, the oscillation amplitude is significantly smaller than the mean flow rate ensuring the counterflow flow configuration remains undisturbed as no flow reversal was observed.

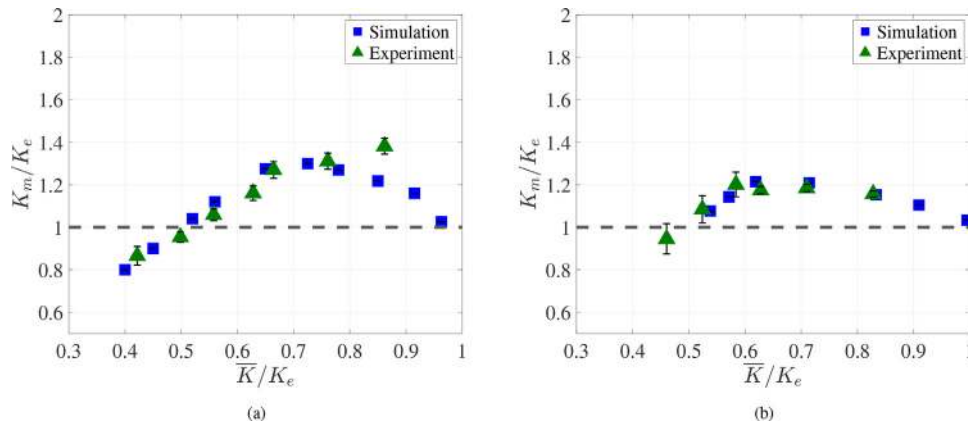


Fig. 8. Comparison of Normalized oscillating strain rate, K_m/K_e as a function of normalized mean strain rate \bar{K}/K_e obtained from simulation, and experiments; (a) $Le > 1$, Flame 1 (b) $Le \leq 1$, Flame 2.

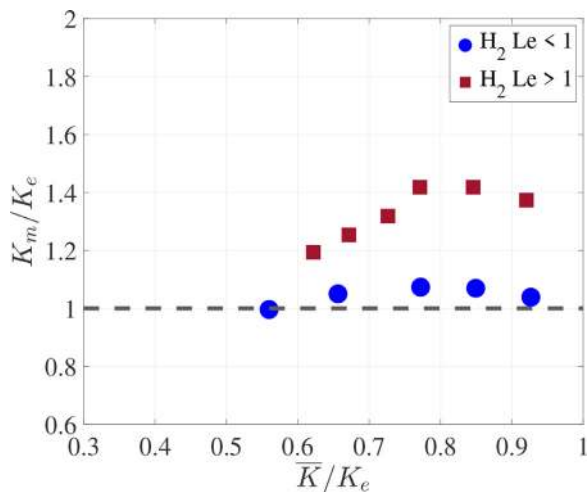


Fig. 9. Comparison of Normalized oscillating strain rate, K_m/K_e as a function of normalized mean strain rate \bar{K}/K_e obtained from simulation for Hydrogen flames.

Additionally, to delineate the maximum instantaneous strain rate experienced by the flame, we plot K_m/K_e as a function of \bar{K}/K_e in Fig. 4b. We observe a monotonic increase in K_m for low mean strain rates (*extinction with flow reversal*), and subsequently becomes almost constant at higher mean strain rates. It is noted that, for almost all data points with $\bar{K}/K_e > 0.5$, K_m/K_e is greater than unity, showing that the $Le > 1$ flames can withstand an instantaneous strain rate higher than their steady state extinction value. This behavior will be discussed further in Section 4. Additionally, the differences in K_o and K_m between two frequencies shown in Fig. 4a and b can be attributed to reduction in perturbation time scale with increase in frequency. This, in turn, weakens the ability of the flame to respond to the perturbation. Thus, the flame under higher forcing frequency can withstand greater extent of strain rate oscillation specifically for $Le > 1$ mixtures. A detailed investigation of frequency dependence will be performed in our next study. The aforementioned extinction characteristics of $Le > 1$ flames under oscillating strain rate for lean CH_4 flames, were also observed for lean C_3H_8 flames (Flame 3, $Le > 1$) as shown in Fig. 5 confirming that such behavior is not fuel-specific.

3.2.2. $Le \leq 1$ flames

Figure 6a shows changes in the normalized amplitude of strain rate needed for extinction (K_o/\bar{K}) as function of normalized mean

strain rate (\bar{K}/K_e) for $Le \leq 1$ mixtures (Flame 2). Similar to $Le > 1$ for $K/K_e < 0.6$, K_o/\bar{K} values are greater than 0.8 and correspond to *extinction due to flow reversal* and are clearly marked in Fig. 6a. For $K/K_e > 0.6$, an approximately linear decrease in amplitude with mean strain rate suggests that extinction was achieved within a small range of maximum instantaneous strain rate. This was confirmed in Fig. 6b, which shows that K_m/K_e is almost constant for all frequencies and \bar{K}/K_e with a slight decrease observed as \bar{K} approached K_e . We also note that $K_m/K_e \approx 1$ which is the steady state extinction strain rate. This is markedly different from the behavior of $Le > 1$ flames, which show $K_m/K_e > 1$. This behaviour is also independent of the specific fuel as evidenced in Fig. 7 for propane flame (Flame 4), with $Le \leq 1$.

4. Numerical simulations and discussion

From experimental observations presented in Section 3, it is apparent that the premixed flames under periodic oscillation of strain rate display distinct behaviors depending on the Lewis number of the mixture. In particular, we found that $Le > 1$ flames can sustain instantaneous strain rates greater than the steady state extinction strain rates of the flame, as expressed by $K_m/K_e > 1$. On the other hand, for $Le \leq 1$ mixture, the maximum instantaneous strain rate a flame can withstand during the oscillations is close to the steady state extinction strain rate ($K_m/K_e \approx 1$). Since such contrasting behavior was observed irrespective of the fuel (CH_4 and C_3H_8) and the frequency (50 and 100 Hz), it is inferred to be the characteristics of $Le >$ and ≤ 1 flames under oscillatory strain rates. To explore such dynamics in detail, we have used the unsteady 1-D counterflow simulations using the OPUS code.

To demonstrate the role of Le on flame response, simulations were carried out for unsteady strain rates at $f = 100$ Hz, for methane flames (Flame 1 and Flame 2) and for hydrogen flames (Flame 5 and Flame 6). First, to check the validity of the simulations, results of OPUS were compared to the corresponding experimental findings for Flame 1 and Flame 2. In particular, numerically computed normalized maximum strain rate (K_m/K_e) observed within a cycle at extinction at various normalized mean strain rate (\bar{K}/K_e) are compared with that of the observed experimental data in Fig. 8. For both the $Le > 1$ (Fig. 8a) and $Le \leq 1$ (Fig. 8b) mixtures, we observe close similarity between numerical and experimental results. Since the Le of methane flames (Flame 1 and 2) are not significantly off-unity (Table 1), we performed additional simulation of unsteady rich (Flame 5) and lean (Flame 6) hydrogen flames, whose Le are significantly greater and smaller than unity,

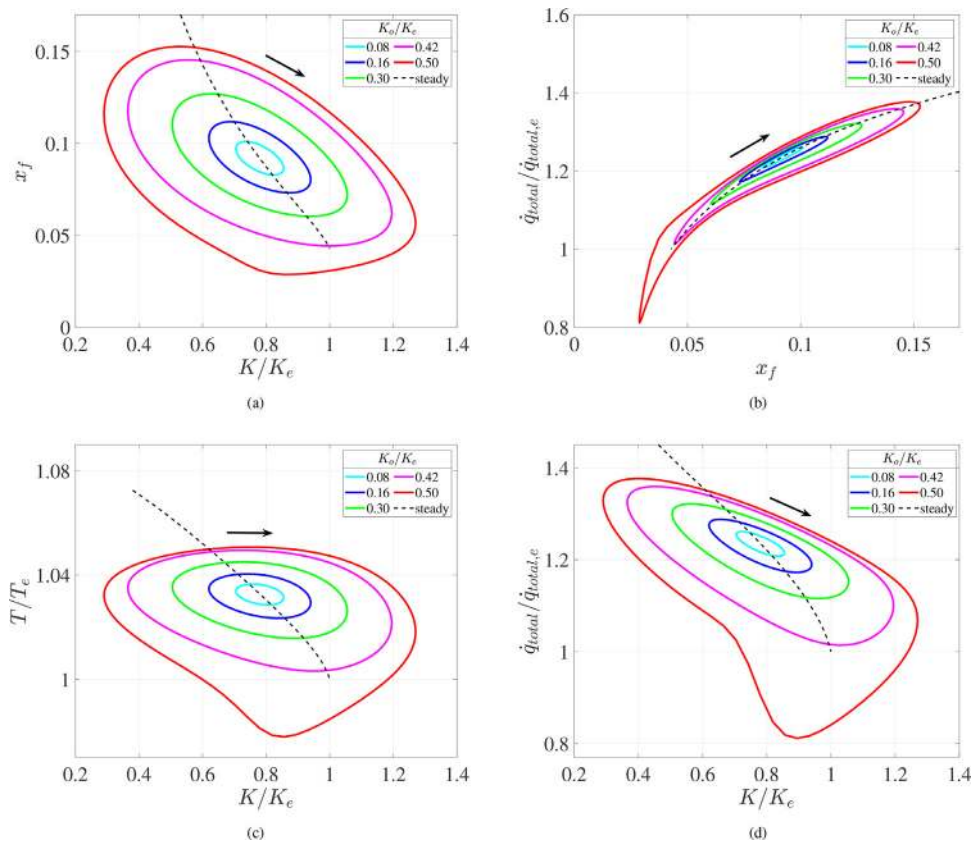


Fig. 10. CH₄, $Le > 1$ flame (Flame 1), Simulation of response to oscillating strain rate for $\bar{K}/K_e = 0.78$; a) Location of downstream flame edge (x_f), as a function of normalized instantaneous strain rate K/K_e . b) Total heat release rate normalized with extinction value ($\dot{q}_{total}/\dot{q}_{total,e}$), as a function of location of downstream flame edge normalized by half separation distance, x_f . c) Flame temperature normalized by steady state extinction value (T/T_e), as a function of K/K_e . d) Total heat release rate normalized with extinction value ($\dot{q}_{total}/\dot{q}_{total,e}$), as a function of normalized instantaneous strain rate K/K_e . The dashed lines in (c) and (d) show the steady state flame response.

respectively (Table 1). These additional simulations illustrate flame dynamics and further clarify that their extinction is a function of Lewis number and independent of specific fuel. As evidenced in Figs. 9, 11 and 13 and further elaborated in later sections, the maximum strain rate threshold of unsteady lean (rich) hydrogen flames mimics that of lean (rich) methane flames given that their Lewis numbers are less (greater) than unity.

Before we present the dynamics of flame response under oscillatory strain rate, we reiterate the steady flame response for mixture with non-unity Le . For both sets of Le , the steady state extinction of flames is foreshadowed by a decrease in the total heat release rate (\dot{q}_{total}) and consequently flame temperature (T) [15]. Figure 3 clearly shows this weakening of steady state flames for Flame 1 and Flame 2. However, the weakening of flames with increasing strain is caused by two distinct phenomena for $Le >$ and ≤ 1 flames. As discussed in Section 3.1, an increase in strain rate weakens $Le > 1$ flames due to increase in heat loss due to thermal diffusion and decrease in incoming species due to mass diffusion. At sufficiently high strain rate, \dot{q}_{total} is too low to sustain a steady flame and this triggers extinction [4,5,9]. On the other hand, the $Le < 1$ flames are strengthened by stretch, so increasing in strain rate causes an increase in flame temperature and heat release, along with the flame migrating to the stagnation plane. As the flame is restricted by the stagnation plane, its thickness and thus residence time is constrained, which causes incomplete reaction leading to decrease in \dot{q}_{total} and eventual extinction [4,5,9,11,31]. It is also important to note that extinction of $Le \approx 1$ is also caused due to insufficient residence time and incomplete reaction. We will see the phenomenon of steady state extinction is key to explain the dichotomy of the extinction conditions ob-

served for $Le >$ and ≤ 1 flames display under oscillatory strain rate.

To demonstrate the dynamical changes in flame response during the oscillations in strain rates, we analyze the phase portraits. In particular, the variation of flame location (x_f), normalized total heat release rate ($\dot{q}_{total}/\dot{q}_{total,e}$), and normalized maximum flame temperature (T/T_e) with the variation of normalized strain rate (K/K_e) for $Le > 1$ flames at a fixed mean strain rate (\bar{K}/K_e) is displayed in Figs. 10 and 11 for Flame 1 ($\bar{K}/K_e = 0.85$) and Flame 5 ($\bar{K}/K_e = 0.77$) respectively. Here x_f is defined as the axial distance between the stagnation plane and the location of maximum heat release rate. All steady state extinction quantities reported, K_e , T_e and $\dot{q}_{total,e}$ are defined for a stable flame just before extinction. First, we note that each phase portrait exhibits a hysteresis in that flame response (flame location, heat release and flame temperature), in that two different trajectories were observed during increasing and decreasing halves of the strain rate oscillations, this manifests in the phase portraits as distortion of the elliptical trajectory.

We also see that, at a smaller amplitude of oscillation ($K_0/K_e < 0.5$), as the instantaneous strain rate increases during the cycle, the total heat release rate and the maximum flame temperature decrease. Simultaneously, the flame migrates closer to the stagnation plane (marked by $x_f = 0$). Such weakening of the $Le > 1$ flames with increased strain rate is expected and was observed for steady state as well (Figs. 10b, c and 11 b, c). Furthermore, during the oscillation, as the instantaneous strain rate approaches and exceeds the steady state extinction value ($K/K_e = 1$), the changes in the heat release and flame temperature become weaker. However, it never reaches the critical value required for extinction. Since the

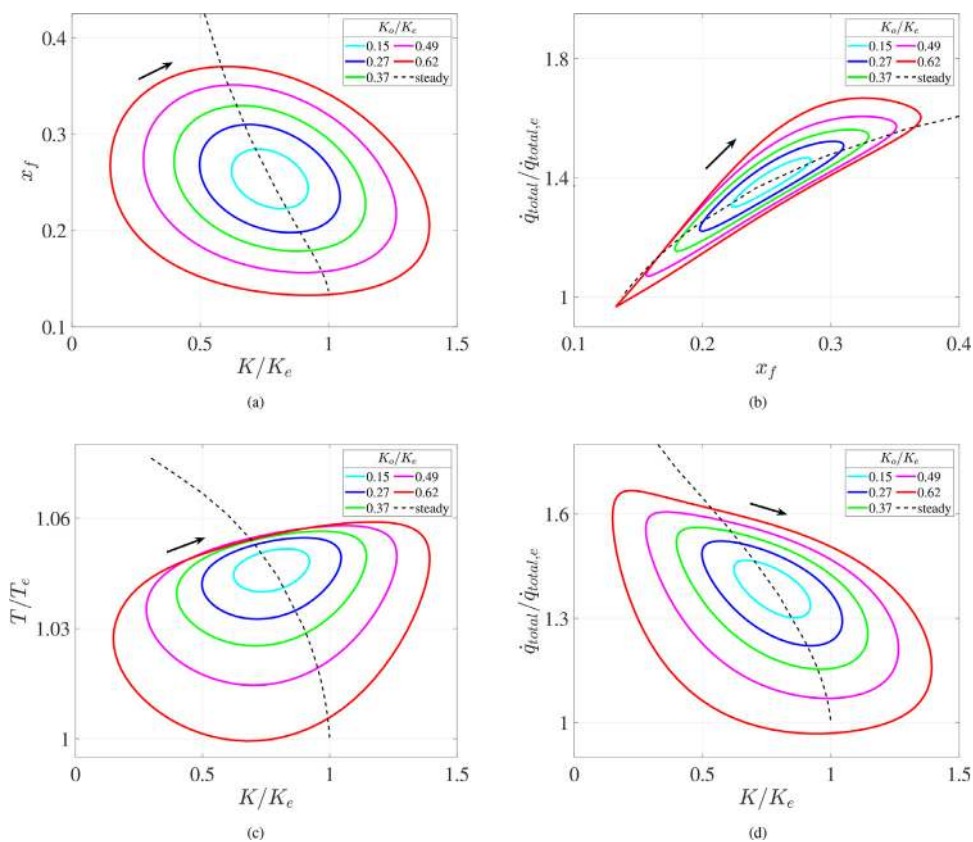


Fig. 11. H₂, Le > 1 flame (Flame 5), Simulation of response to oscillating strain rate for $\bar{K}/K_e = 0.77$; a) Location of downstream flame edge (x_f), as a function of normalized instantaneous strain rate K/K_e . b) Total heat release rate normalized with extinction value ($\dot{q}_{total}/\dot{q}_{total,e}$), as a function of location of downstream flame edge normalized by half separation distance, x_f . c) Flame temperature normalized by steady state extinction value (T/T_e), as a function of K/K_e . d) Total heat release rate normalized with extinction value ($\dot{q}_{total}/\dot{q}_{total,e}$), as a function of normalized instantaneous strain rate K/K_e . The dashed lines in (c) and (d) show the steady state flame response.

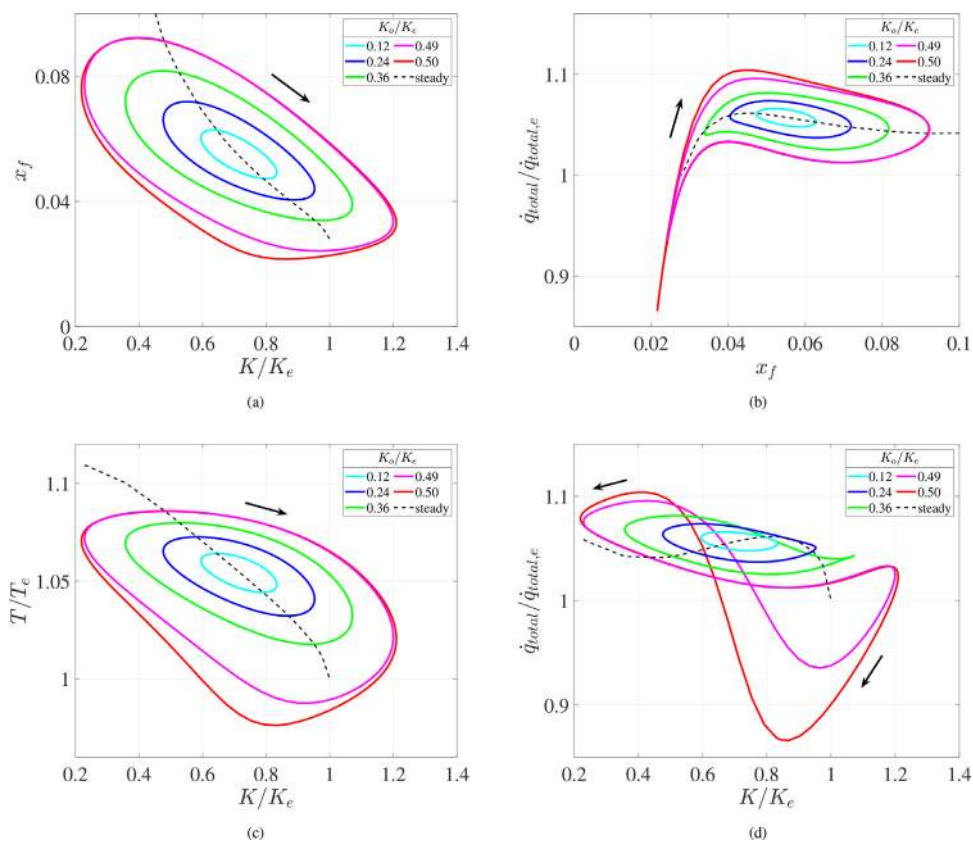


Fig. 12. CH₄, Le ≤ 1 flame (Flame 2), Simulation of response to oscillating strain rate for $\bar{K}/K_e = 0.71$; (a) Location of downstream flame edge (x_f), as a function of normalized instantaneous strain rate K/K_e . (b) Total heat release rate normalized with extinction value ($\dot{q}_{total}/\dot{q}_{total,e}$), as a function of location of downstream flame edge normalized by half separation distance, x_f . (c) Flame temperature normalized by steady state extinction value (T/T_e), as a function of K/K_e . (d) Total heat release rate normalized with extinction value ($\dot{q}_{total}/\dot{q}_{total,e}$), as a function of normalized instantaneous strain rate K/K_e . The dashed lines in (c) and (d) show the steady state flame response.

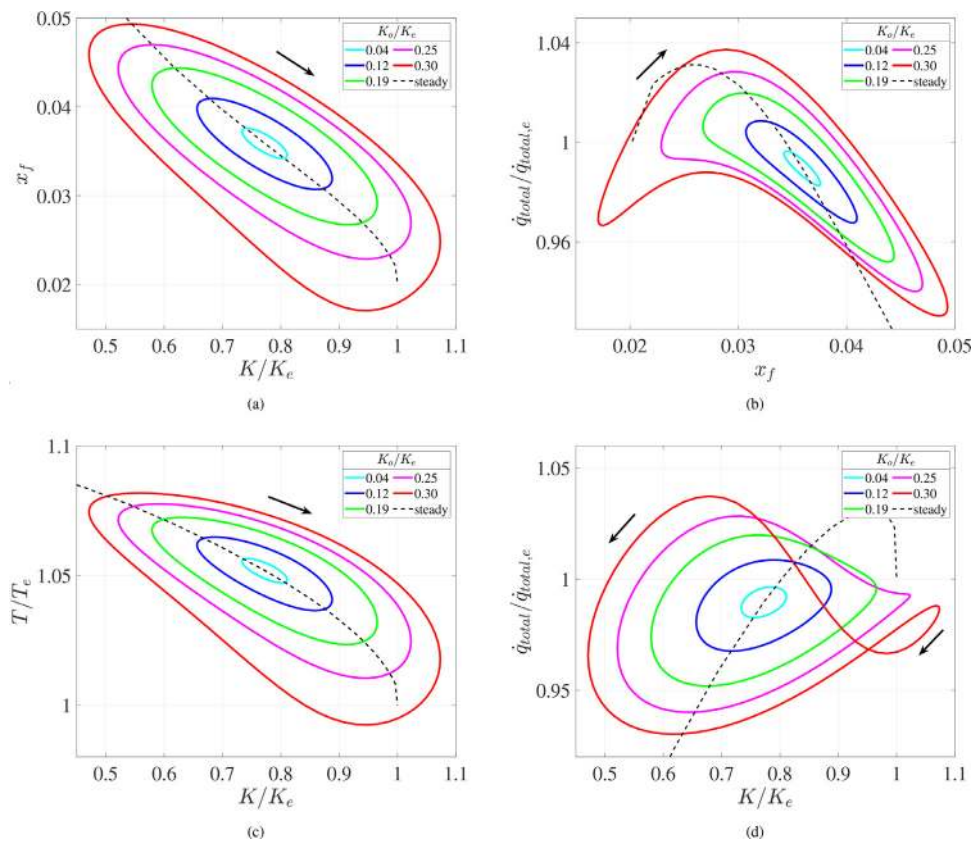


Fig. 13. H_2 , $Le < 1$ flame (Flame 6), Simulation of response to oscillating strain rate for $\bar{K}/K_e = 0.77$; (a) Location of downstream flame edge (x_f), as a function of normalized instantaneous strain rate K/K_e . (b) Total heat release rate normalized with extinction value ($\dot{q}_{total}/\dot{q}_{total,e}$), as a function of location of downstream flame edge normalized by half separation distance, x_f . (c) Flame temperature normalized by steady state extinction value (T/T_e), as a function of K/K_e . (d) Total heat release rate normalized with extinction value ($\dot{q}_{total}/\dot{q}_{total,e}$), as a function of normalized instantaneous strain rate K/K_e . The dashed lines in (c) and (d) show the steady state flame response.

flame is located far from the stagnation plane (noted by $x_f = 0$), the flame is essentially free to move and adjusts its location as it maintains kinematic balance between flame speed and flow velocity during the cycle. Such a change in flame location temporally strengthens the flame as seen by the slight increase in temperature and heat release as the instantaneous strain rate exceeds steady state extinction value. This mechanism allows the $Le > 1$ to withstand periodic oscillation, where instantaneous strain rate for a section of the cycle is greater than the steady state extinction. With further increase in the oscillation amplitude (K_o/K_e), a gradual decrease in total heat release rate was observed until the minimum flame temperature during the cycle reaches the critical value of (approximately) steady state extinction and unable to recover, and the flame extinguishes. Note that even though the Le values for Flame 1 and Flame 5 (1.11 and 1.97) are significantly different, the extinction mechanism of these $Le > 1$ flames under strain rate oscillations is nearly identical, as evidenced in Figs. 10 and 11.

On the other hand, the phase portraits for $Le \leq 1$ flames present a largely different behavior as shown in Fig. 12 for $\bar{K}/K_e = 0.71$ for Flame 2 and, Fig. 13 for $\bar{K}/K_e = 0.77$ for Flame 6. The steady state extinction for $Le \leq 1$ flames are strongly coupled to the proximity of the flame to the stagnation plane. Similarly, we observe a strong effect of instantaneous flame location on the total heat release and flame temperature during the strain rate oscillations as shown in phase portraits (Fig. 12). An increase in instantaneous strain rate consistently pushes the flame towards the stagnation plane, and, unlike for $Le > 1$ flames, this flame fails to move and adjust to a favourable condition. As a result, due to decrease in the residence time and resulting incomplete reaction, the flame temperature and total heat release suddenly drop during the cycle, as

shown in Figs. 12 and 13, a behavior also reported in Stahl and Warnatz [30]. This drastic drop in heat release and accompanying decrease in flame temperature ultimately causes extinction, when amplitude of strain rate is increased. Since the extinction of $Le \leq 1$ flames is caused by the immobility of the flame from the stagnation plane, which occurs at $K \approx K_e$, the maximum strain rate in a cycle remains close to extinction condition, $K_m \approx K_e$.

5. Conclusion

In summary, we presented a study on the effects of oscillation in upstream flow on the extinction strain rates for premixed flames with non-unity Le . Using premixed counterflow twin-flames, we showed that for $Le > 1$ flames, the maximum instantaneous strain rate exceeds the steady state extinction strain rate, and hence, extinction is delayed. This observation was subsequently supported with unsteady numerical simulations. We showed that the total heat release rate of an unsteady $Le > 1$ flame decreases gradually with an increase in mean strain rate, and thus, the flame continuously adjusts its position. Such mobility allows the flame to maintain its temperature above a critical limit, although the instantaneous strain rates are greater than the steady state extinction condition. Extinction eventually occurs when the total heat release is significantly lowered and the flame temperature drops below its critical value.

For $Le \leq 1$ flames, however, the flame extinction is controlled by the lack of residence time and the consequent incomplete combustion, and hence critical strain rate for extinction is bounded by its steady state value. Such a flame shows an abrupt decrease in heat release rate as the instantaneous strain rate during the cy-

cle approaches the steady state extinction condition. At this point, the flame loses its mobility as it approaches the stagnation plane and hence experiences limited residence time. Thus, the maximum strain rate barely exceeds the steady state extinction condition.

We end the exposition by recognizing that the dichotomy in the extinction behavior for $Le >$ and ≤ 1 flames mentioned above can be observed for high mean strain rates. For low mean strain rates, the amplitude of oscillation required for extinction exceeds the mean strain rate values, and as such, flow reversal occurs. Such reversal in the flow direction causes the flame to be destabilized, leading the flame to undergo *extinction due to flow reversal* irrespective of Le .

Declaration of Competing Interest

The authors declare that they have no known competing financial interests or personal relationships that could have appeared to influence the work reported in this paper.

Acknowledgments

The authors are grateful to Prof. Chung K. Law from Princeton University for stimulating discussions and comments on the manuscript. The authors would like to thank Mr. Takuya Tomidokoro, at Keio University, for his assistance with OPUS code. The research was supported by the internal grants from Jacobs School of Engineering at UC San Diego.

References

- [1] N. Peters, Laminar flamelet concepts in turbulent combustion, *Proc. Combust. Inst.* 21 (1) (1988) 1231–1250.
- [2] P.A. Libby, F.A. Williams, Structure of laminar flamelets in premixed turbulent flames, *Combust. Flame* 44 (1–3) (1982) 287–303.
- [3] P.A. Libby, F.A. Williams, Strained premixed laminar flames under nonadiabatic conditions, *Combust. Sci. Technol.* 31 (1–2) (1983) 1–42.
- [4] H. Tsuji, I. Yamaoka, Structure and extinction of near-limit flames in a stagnation flow, *Proc. Combust. Inst.* 19 (1) (1982) 1533–1540.
- [5] S. Ishizuka, C.K. Law, An experimental study on extinction and stability of stretched premixed flames, *Proc. Combust. Inst.* 19 (1) (1982) 327–335.
- [6] I. Yamaoka, H. Tsuji, Determination of burning velocity using counterflow flames, *Proc. Combust. Inst.* 20 (1) (1985) 1883–1892.
- [7] J. Sato, Effects of lewis number on extinction behavior of premixed flames in a stagnation flow, *Proc. Combust. Inst.* 19 (1) (1982) 1541–1548.
- [8] J.H. Tien, M. Matalon, On the burning velocity of stretched flames, *Combust. Flame* 84 (3–4) (1991) 238–248.
- [9] C.K. Law, D.L. Zhu, G. Yu, Propagation and extinction of stretched premixed flames, *Proc. Combust. Inst.* 21 (1) (1988) 1419–1426.
- [10] C.K. Law, Dynamics of stretched flames, *Proc. Combust. Inst.* 22 (1) (1989) 1381–1402.
- [11] C.K. Law, C. Sung, G. Yu, R. Axelbaum, On the structural sensitivity of purely strained planar premixed flames to strain rate variations, *Combust. Flame* 98 (1–2) (1994) 139–154.
- [12] M. Kitano, Y. Otsuka, On flammability limits and flame shapes of counterflow premixed flames, *Combust. Sci. Technol.* 48 (5–6) (1986) 257–271.
- [13] F. Egolfopoulos, C.K. Law, Chain mechanisms in the overall reaction orders in laminar flame propagation, *Combust. Flame* 80 (1) (1990) 7–16.
- [14] C.K. Law, F. Egolfopoulos, A unified chain-thermal theory of fundamental flammability limits, *Symp. (Int.) Combust.* 24 (1) (1992) 137–144.
- [15] C.K. Law, *Combustion Physics*, Cambridge University Press, 2010.
- [16] H.G. Pearlman, S.H. Sohrab, Extinction of counterflow premixed flames under periodic variation of the rate of stretch, *Combust. Sci. Technol.* 105 (1–3) (1995) 19–31.
- [17] N. Darabiha, Transient behaviour of laminar counterflow hydrogen-air diffusion flames with complex chemistry, *Combust. Sci. Technol.* 86 (1–6) (1992) 163–181.
- [18] E.J. Welle, W.L. Roberts, C.D. Carter, J.M. Donbar, The response of a propane-air counter-flow diffusion flame subjected to a transient flow field, *Combust. Flame* 135 (3) (2003) 285–297.
- [19] G. Bansal, H.G. Im, J.K. Bechtold, Flame-flow interactions and flow reversal, *Combust. Flame* 159 (4) (2012) 1489–1498.
- [20] F.N. Egolfopoulos, C.S. Campbell, Unsteady counterflowing strained diffusion flames: diffusion-limited frequency response, *J. Fluid Mech.* 318 (1996) 1–29.
- [21] A. Cuoci, A. Frassoldati, T. Faravelli, E. Ranzi, Extinction of laminar, premixed, counter-flow methane/air flames under unsteady conditions: effect of H_2 addition, *Chem. Eng. Sci.* 93 (2013) 266–276.
- [22] G. Joulin, On the response of premixed flames to time-dependent stretch and curvature, *Combust. Sci. Technol.* 97 (1–3) (1994) 219–229.
- [23] H.G. Im, J.H. Chen, Effects of flow transients on the burning velocity of laminar hydrogen/air premixed flames, *Proc. Combust. Inst.* 28 (2) (2000) 1833–1840.
- [24] T. Hirasawa, T. Ueda, A. Matsuo, M. Mizomoto, Effect of oscillatory stretch on the flame speed of wall-stagnating premixed flame, *Proc. Combust. Inst.* 27 (1) (1998) 875–882.
- [25] T. Brown, R. Pitz, C. Sung, Oscillatory stretch effects on the structure and extinction of counterflow diffusion flames, *Symp. (Int.) Combust.* 27 (1) (1998) 703–710.
- [26] F. Zhang, T. Zirwes, P. Habisreuther, H. Bockhorn, Effect of unsteady stretching on the flame local dynamics, *Combust. Flame* 175 (2017) 170–179.
- [27] T. Zirwes, F. Zhang, Y. Wang, P. Habisreuther, J.A. Denev, Z. Chen, H. Bockhorn, D. Trimis, In-situ flame particle tracking based on barycentric coordinates for studying local flame dynamics in pulsating bunsen flames, *Proc. Combust. Inst.* 38 (2) (2021) 2057–2066.
- [28] H.G. Im, J.K. Bechtold, C.K. Law, Response of counterflow premixed flames to oscillating strain rates, *Combust. Flame* 105 (3) (1996) 358–372.
- [29] M.E. Decroix, W.L. Roberts, Study of transient effects on the extinction limits of an unsteady counterflow diffusion flame, *Combust. Sci. Technol.* 146 (1–6) (1999) 57–84.
- [30] G. Stahl, J. Warnatz, Numerical investigation of time-dependent properties and extinction of strained methane and propane-air flamelets, *Combust. Flame* 85 (3–4) (1991) 285–299.
- [31] C.J. Sung, C.K. Law, Structural sensitivity, response, and extinction of diffusion and premixed flames in oscillating counterflow, *Combust. Flame* 123 (3) (2000) 375–388.
- [32] J. Kistler, C. Sung, T. Kreut, C.K. Law, M. Nishioka, Extinction of counterflow diffusion flames under velocity oscillations, *Symp. (Int.) Combust.* 26 (1) (1996) 113–120.
- [33] N. Peters, *Turbulent Combustion*, Cambridge University Press, 2004.
- [34] H. Chelliah, C.K. Law, T. Ueda, M. Smooke, F. Williams, An experimental and theoretical investigation of the dilution, pressure and flow-field effects on the extinction condition of methane-air-nitrogen diffusion flames, *Symp. (Int.) Combust.* 23 (1) (1991) 503–511.
- [35] U. Niemann, K. Seshadri, F.A. Williams, Accuracies of laminar counterflow flame experiments, *Combust. Flame* 162 (4) (2015) 1540–1549.
- [36] M. Matalon, On flame stretch, *Combust. Sci. Technol.* 31 (3–4) (1983) 169–181.
- [37] F.N. Egolfopoulos, N. Hansen, Y. Ju, K. Kohse-Höinghaus, C.K. Law, F. Qi, Advances and challenges in laminar flame experiments and implications for combustion chemistry, *Prog. Energy Combust. Sci.* 43 (2014) 36–67.
- [38] H.G. Im, L.L. Raja, R.J. Kee, A.E. Lutz, L.R. Petzold, OPUS: A Fortran program for unsteady opposed-flow flames (2000).
- [39] A.E. Lutz, R.J. Kee, J.F. Grcar, F.M. Rupley, OPDIF: a Fortran program for computing opposed-flow diffusion flames, Technical Report, Sandia National Labs., Livermore, CA (United States), 1997.
- [40] Li, S., Petzold, L. (1999). Design of new DASPK for sensitivity analysis. UCSB Department of Computer Science Technical Report. It is a technical report published by UC Santa Barbara Department of Computer Science Technical Report. URL: <https://cs.ucsb.edu/research/tech-reports/1999-28>.
- [41] U.M. Ascher, L.R. Petzold, *Computer Methods for Ordinary Differential Equations and Differential-Algebraic Equations*, SIAM, 1998.
- [42] R.J. Kee, F.M. Rupley, J.A. Miller, *Chemkin-II: A Fortran chemical kinetics package for the analysis of gas-phase chemical kinetics*, Technical Report, Sandia National Lab.(SNL-CA), Livermore, CA (United States), 1989.
- [43] R.J. Kee, G. Dixon-Lewis, J. Warnatz, M.E. Coltrin, J.A. Miller, A Fortran computer code package for the evaluation of gas-phase multicomponent transport properties, Sandia National Laboratories Report, 1986, 80401–1887.
- [44] G.P. Smith, D.M. Golden, M. Frenklach, N.W. Moriarty, B. Eiteneer, M. Goldenberg, C.T. Bowman, R.K. Hanson, S. Song, W. Jr. Gardiner, et al., GRI-Mech 3.0, URL http://www.me.berkeley.edu/gri_mech (1999).
- [45] T. Tomidokoro, T. Yokomori, H.G. Im, T. Ueda, Characteristics of counterflow premixed flames with low frequency composition fluctuations, *Combust. Flame* 212 (2020) 13–24.
- [46] T. Tomidokoro, T. Yokomori, T. Ueda, H.G. Im, A computational analysis of strained laminar flame propagation in a stratified CH_4/H_2 /air mixture, *Proc. Combust. Inst.* 38 (2) (2021) 2543–2550.
- [47] E.R. Hawkes, J.H. Chen, Comparison of direct numerical simulation of lean premixed methane-air flames with strained laminar flame calculations, *Combust. Flame* 144 (1–2) (2006) 112–125.
- [48] H.G. Im, L.L. Raja, R.J. Kee, L.R. Petzold, A numerical study of transient ignition in a counterflow nonpremixed methane-air flame using adaptive time integration, *Combust. Sci. Technol.* 158 (1) (2000) 341–363.
- [49] R. Sankaran, H.G. Im, Dynamic flammability limits of methane/air premixed flames with mixture composition fluctuations, *Proc. Combust. Inst.* 29 (1) (2002) 77–84.
- [50] S. Liu, J.C. Hewson, J.H. Chen, H. Pitsch, Effects of strain rate on high-pressure nonpremixed n-heptane autoignition in counterflow, *Combust. Flame* 137 (3) (2004) 320–339.

- [51] R. Seiser, J. Frank, S. Liu, J. Chen, R. Sigurdsson, K. Seshadri, Ignition of hydrogen in unsteady nonpremixed flows, *Proc. Combust. Inst.* 30 (1) (2005) 423–430.
- [52] T. Hirasawa, T. Ueda, A. Matsuo, M. Mizomoto, Response of flame displacement speeds to oscillatory stretch in wall-stagnating flow, *Combust. Flame* 121 (1–2) (2000) 312–322.
- [53] C.J. Sun, C.J. Sung, D.L. Zhu, C.K. Law, Response of counterflow premixed and diffusion flames to strain rate variations at reduced and elevated pressures, *Proc. Combust. Inst.* 26 (1) (1996) 1111–1120.
- [54] F.N. Egolfopoulos, Dynamics and structure of unsteady, strained, laminar premixed flames, *Proc. Combust. Inst.* 25 (1) (1994) 1365–1373.